Ultra-wideband transmitter design based on a new transmitted reference pulse cluster

Yiming Huo, Xiaodai Dong, Ping Lu

September 2017

KICS The Korean Institute of Communications and Information Sciences

Available online at www.sciencedirect.com

ScienceDirect

ICT Express 3 (2017) 142–147

www.elsevier.com/locate/icte

Ultra-wideband transmitter design based on a new transmitted reference pulse cluster☆

Yiming Huo[a,*], Xiaodai Dong[a], Ping Lu[b]

[a] *Department of Electrical and Computer Engineering Department, University of Victoria, Canada*
[b] *Department of Information Technology, LTH, Lund University, Sweden*

Received 18 November 2016; received in revised form 17 April 2017; accepted 3 July 2017
Available online 1 August 2017

Abstract

This study presents an energy efficient ultra-wideband (UWB) transmitter based on the novel transmitted reference pulse cluster (TRPC) modulation scheme. The TRPC-UWB transmitter integrates wideband active baluns, a wideband IQ modulator based on up-conversion mixers, and a differential-to-single-ended converter. The integrated circuits of the TRPC-UWB front end are designed and implemented in a low-cost 130-nm CMOS process. The measured worst-case carrier leakage suppression is 22.4 dBc, whereas the single sideband suppression is greater than 31.6 dBc, operating at a frequency from 3.1 to 8.2 GHz. With an adjustable data rate of 10 to 300 Mbps, the transmitter achieves good energy efficiency of 38.4 pJ/pulse and a maximum current consumption of 24.5 mA from a 1.2-V power supply.

Keywords: Ultra-wideband (UWB); Transmitted reference pulse cluster; IQ modulator; CMOS

1. Introduction

Spectrum has become an increasingly scarce resource as the wireless communication market has grown at an unprecedented pace. The spectrum below 6 GHz becomes very crowded. Ultra-wideband (UWB) technology has emerged as a candidate solution to short-range high data rate communications thanks to its ultra-wide spectrum in the unlicensed 3.1–10.6 GHz band allocated by the Federal Communications Commission (FCC). Impulse radio (IR) is widely used for UWB communications. IR-UWB transmitters were realized by the structures in [1,2] or without a carrier [3]. In these IR-UWB designs, simple modulation schemes such as on–off keying (OOK), binary phase-shift keying (BPSK), and pulse-position modulation (PPM), were employed and demonstrated very good energy efficiency. IR-UWB can be categorized into coherent and non-coherent schemes. Non-coherent schemes generally have much lower complexity, power consumption and cost than coherent schemes. In non-coherent schemes, estimating the long multipath UWB channels at a minimal price of error performance or data rate is not required. Of the non-coherent (NC) schemes, transmitted reference pulse cluster (TRPC) leads in error rate performance, data rate, robustness and ease of implementation [4]. Furthermore, it provides robust performance to time variation and immunity to pulse distortion caused by frequency dependent antenna and channel effects. The baseband equivalent TRPC transmitted signal is:

$$\tilde{s}(t) = \sqrt{\frac{E_b}{2N_P}} \sum_{m=-\infty}^{\infty} \sum_{i=0}^{N_f-1} [g(t - mT_s - 2iT_d) + b_m(t - mT_s - 2iT_d)] \quad (1)$$

where N_p denotes for the number of total pulses in one cluster, E_b is the average energy per bit, $g(t)$ denotes the component pulse of width T_p in a single pulse cluster, T_s denotes the symbol duration, and T_d is the delay among the pulses in a single cluster. Usually $T_d = T_p$ or some multiples of T_p, and

* Corresponding author.
E-mail address: ymhuo@uvic.ca (Y. Huo).
Peer review under responsibility of The Korean Institute of Communications Information Sciences.
☆ This paper has been handled by Prof. Seong-Lyun Kim.

http://dx.doi.org/10.1016/j.icte.2017.07.001

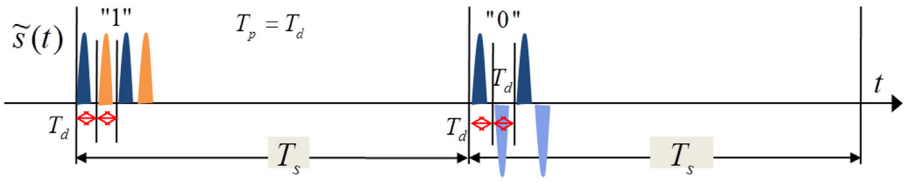

Fig. 1. TRPC structure.

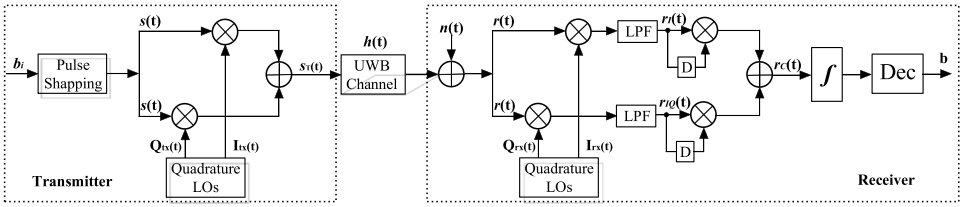

Fig. 2. Block of the proposed TRPC-UWB transceiver.

$T_s \geq N_p T_d + \tau max$, where τmax denotes the maximum channel delay. Fig. 1 illustrates TRPC signal structures, where "1" represents a single pulse cluster that consists of all "positive" pulses, and "0" represents one pulse cluster containing both positive and negative pulses. A simple auto-correlation receiver with short delay lines and a low analog-to-digital sampling rate can successfully collect the transmitted energy that is spread into multipaths without explicit channel estimation. It was shown in [4] that TRPC achieves a 2–3 dB and 1.3–2 dB power gain over conventional TR and NC-PPM schemes. In this study, we present a novel TRPC-UWB transmitter design based on the CMOS transmitter front end [5].

The remainder of this paper is organized as follows. Section 2 describes the transceiver system architecture and derives the transmitter specifications to comply with the FCC UWB emission limit. In Section 3, a detailed circuit design is presented. Section 4 presents experimental results that demonstrate good radio frequency (RF) and energy efficiency performance. A conclusion is provided in Section 5.

2. TRPC-UWB transmitter specification

Fig. 2 shows the main function blocks of a TRPC-UWB transceiver. After pulse shaping, the identical TRPC pulse train *s(t)* is sent to both I and Q branches at the transmitter end. At the receiver end, the UWB signal is down-converted through an IQ demodulator, followed by low-pass filters (LPFs) and auto-correlators. After signal combining, pulse integration, and decimation, the baseband signal is successfully recovered. The mathematical derivation proves that the constant carrier frequency is successfully canceled by using the TRPC scheme and IQ modulation/demodulation architecture [6]. Therefore, the TRPC UWB system is not sensitive to frequency and phase mismatch. Another benefit of using the direct-conversion topology is that it has very pure output without undesired frequency products [7]. These advantages derived from the system level largely alleviate the complexity and difficulty of implementation.

Furthermore, FCC regulates that the effective isotropic radiated power (EIRP) should not exceed −41.25 dBm/MHz, and that the peak EIRP density level should be below 0 dBm in a 50-MHz bandwidth. This prevents the unlicensed UWB signals from interfering with another spectrum. For the TRPC signaling structure, it remains to be discovered whether the component pulse amplitude enables EIRP to comply with the FCC regulation. In a UWB system that employs a single pulse having a pulse width of T_p and a pulse repetition frequency (PRF) of R_p, the relationship between the entire full bandwidth (FBW) peak power and the average power of the UWB signal is indicated by the following equation:

$$P_{ave} = P_{peak} \cdot \delta \tag{2}$$

where P_{peak} is the FBW peak power and $\delta = T_p \cdot R_p$ is the pulse duty cycle. However, because of limited resolution bandwidth (RBW) in the spectrum analyzer measurements, the measured peak and average power vary from the aforementioned theoretical calculations. According to [8], a RBW filter with bandwidth BR leads to the following.

$$P^m_{ave} = P^m_{peak} = (R_P \cdot \tau_R)^2 \cdot P_{peak} \cdot T_p^2 \cdot B_R^2 = P_{peak} \cdot T_p^2 \cdot B_P^2 \quad R_P \gg B_R \tag{3}$$

where P^m_{ave} and P^m_{peak} are the measured average and peak power, respectively, and τ_R is the reciprocal of B_R. Eq. (3) implies that when $R_p \gg B_R$, the RBW filter in the spectrum analyzer effectively sums $R_p \cdot \tau_R$ pulses. Consequently, the amplitude increases by $R_p \cdot \tau_R$ times, and the power by $(R_p \cdot \tau_R)^2$ times. By contrast, TRPC signaling has a unique structure consisting of N_p contiguous pulses, and the cluster repeats at a rate of R, which is much greater than B_R. Following a similar argument in [9], the output of the spectrum analyzer is the sum of the $N_p \cdot R \cdot \tau_R$ component pulses. Thus, the measured average and peak power are given by

$$P^m_{ave} = P^m_{peak} = (N_P \cdot R \cdot \tau_R)^2 \cdot P_{peak} \cdot T_p^2 \cdot B_R^2 = N_p^2 \cdot P_{peak} \cdot T_p^2 \cdot R^2 R \gg B_R. \tag{4}$$

In this study, the designed data rate ranges from 10 to 300 Mbps, which is much larger than the RBW of 1 MHz. Moreover, (4) indicates that the measured power will increase by

Table 1
Pulse cluster design specification.

Data Rate (Mbps)	N_P	T_P (ns)	BW_{3-dB} (MHz)	$P_{Peak,RRC}$ (dBm)	Max. Amp. (mV)
10	8	1.65	650	−23.47	32.8
20	8	1.65	650	−29.47	16.4
40	8	0.85	1180	−29.47	16.4
100	4	0.85	1180	−31.93	12.36
200	4	0.85	1180	−37.9	6.21
250	3	0.85	1180	−37.3	6.63
300	2	0.85	1180	−35.4	8.28

6.02 dB when the number of the pulses doubles. By referring to the FCC UWB emission limit, the measured average EIRP and peak EIRP should meet the following requirement below.

$$P_{\text{peak}}^{\text{m}} \leq -41.25 \text{ dBm or } 75 \text{ nW in 1 MHz RBW} \quad (5)$$

$$P_{\text{peak}}^{\text{m}} \leq \left(\frac{B_R}{50 \times 10^6}\right) \text{mW or } 10^6 \leq B_R \leq 50 \times 10^6. \quad (6)$$

That the TRPC-UWB transmission power is an FCC average power constrained is apparent, and we can calculate P_{peak} to ensure (4) meets the condition in (5). Next, the amplitude of a component pulse in TRPC is found from the obtained P_{peak} and the actual pulse shape. In this study, the TRPC signaling employs root raised cosine (RRC) pulses to form a cluster. The normalized RRC pulse is given by:

$$g(t) = \frac{\cos[(1+\beta)\pi t/T] + \frac{\sin[(1-\beta)\pi t/T]}{4\beta t/T}}{1-(4\beta t/T)^2} \quad (7)$$

where β is roll-off factor and equals 0.25 in this work. When $g(t)$ is modulated by a local oscillator (LO) signal, the up-converted signal has a time-domain expression of:

$$s(t) = A_{TX} \cdot g(t) \cdot \cos(\omega_{LO} \cdot t) \quad (8)$$

where A_{TX} is the amplitude of the output carrier modulated pulse, which has a unit of voltage and depends on the overall gain of the entire transmitter, the pulse amplitude, and the strength of the LO signal. The measured FBW power peak of this TRPC component pulse at the receiver (RX) end is therefore formulated as

$$P_{\text{Peak, RRC}} = \int_{-\frac{T_P}{2}}^{\frac{T_P}{2}} \frac{S^2(t)}{Z_{load} \cdot T_P} dt \quad (9)$$

where Z_{load} is the load impedance of the instrument or antenna at the RX end, and is ideally 50 ohms.

Finally, the exact amplitude A_{TX} of the TRPC-UWB output signal that fully complies with the FCC UWB emission limit is mathematically derived and summarized in Table 1. The maximum amplitudes of the output signal indicate that the overall transmitter gain should be comparatively small and tunable, considering that the typical peak-to-peak amplitude of the LO signal is 1 V.

3. Detailed transmitter design

As shown in Fig. 3, the baseband pulse cluster, which occupies a bandwidth from DC to more than 1200 MHz is directly fed into the wideband active baluns on the I and Q paths. The double-balanced up-conversion mixers based IQ modulator realizes the frequency up-conversion. Finally, the up-converted differential RF signals are transformed to single-ended ones through a differential-to-single-ended (D-to-S) converter with a variable gain control. The DC offset in the baseband input causes the growth of carrier leakage, which not only deteriorates the error vector magnitude (EVM) but also elevates the emission level close to the FCC UWB mask.

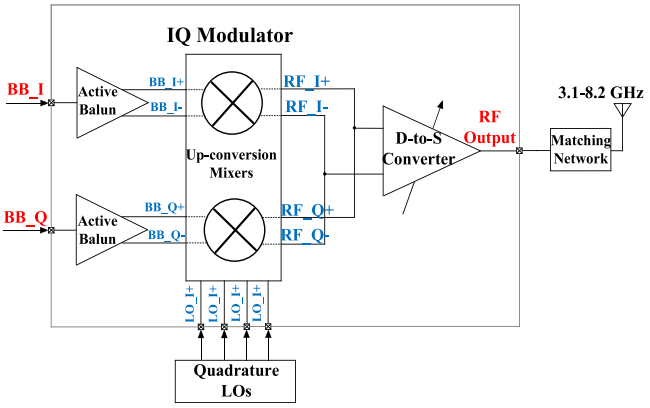

Fig. 3. Block diagram of the TRPC-UWB TX front end.

3.1. Wideband active balun

Passive balun normally occupies a large physical area and introduces front-end loss, which increases NF. Therefore, a low-noise active balun is designed to transform the single-ended baseband signal to differential ones. As depicted in Fig. 4, the poly-resistors provide biasing, and the input signals are separated into two paths. In the first path, M1, M3, and R1 form a common-gate (CG) amplifier with an NMOS current source; the CG has a positive voltage gain. In the second path, a cascode structure is configured. M4 is the input device configured in the CS stage, and M2 forms the CG stage. The two paths are separated by C2, which functions as both DC blocking and phase/amplitude compensation. By using this topology, both the noise and distortion of the CG transistor are canceled [10].

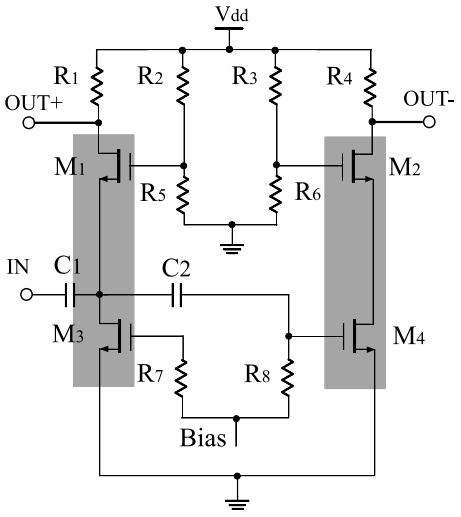

Fig. 4. Wideband balun with amplifying stages highlighted.

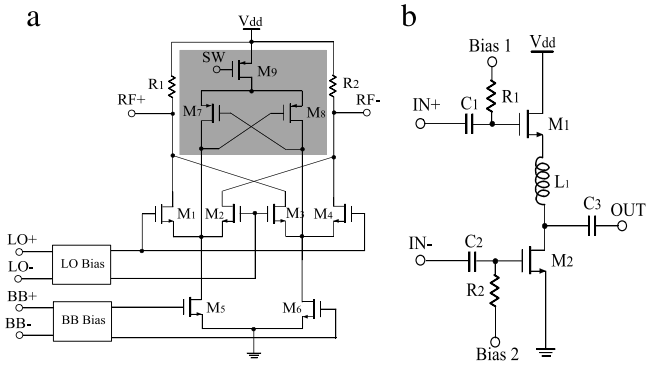

Fig. 5. (a) Up-conversion mixer and (b) D-to-S converter.

3.2. Up-conversion mixer

An up-conversion mixer has a critical impact on the entire system EVM. Here, a double-balanced Gilbert is designed thanks to the merits of low even-order distortion products, a high-input second-order intercept point (IIP2), and good isolation among ports. As illustrated in Fig. 5(a), an up-conversion mixer consists of an input trans-conductance stage, LO switches, and passive loads. A quasi-differential pair with the source touched to AC ground must complete the trans-conductance stage, as this topology can achieve a good third-order intercept point (IP3).

PMOS transistors M7, M8 and M9 dynamically inject the current into M5 and M6 only when the zero-crossing of the LO signal occurs. Therefore, the LO signal is biased at a certain voltage, which makes only M3 to conduct during zero-crossing. The current injection technique considerably reduces the flicker noise translated to the RF output. It also increases the bias current of M5 and M6 without changing the bias current of M1, M2, M3, and M4 [11]. Therefore, the IP3 performance also improves.

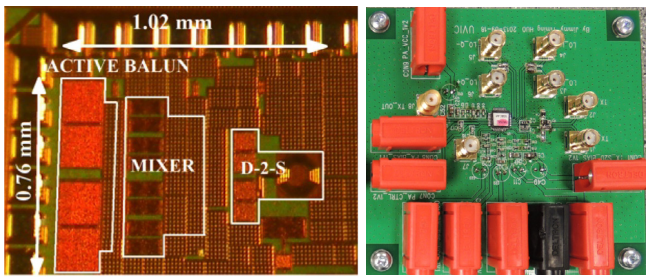

Fig. 6. Transmitter chip and test PCB board.

3.3. Differential-to-single-ended converter

The differential-to-single-ended (D2S) converter finally combines the differential RF signals to the single-ended ones with a tunable gain controlled by the biasing voltage. By using the current sharing technology, the maximum current consumption is reduced to less than 4 mA. As shown in Fig. 5(b), the inductor L_1 functions as a peaking element resonant with the parasitic capacitor at the output of the D2S converter.

4. Fabrication and measurement results

The transmitter front-end chip is fabricated in a cost-effective IBM 130-nm CMOS process as shown in Fig. 6. This process provides special optimization for RF design. The total area is approximately 0.55 mm^2, and the TRPC-UWB PCB board is designed in low-cost FR-4 material. For verification, as shown in Fig. 7(c), a Tektronix 7052 arbitrary waveform generator (AWG) is programmed to generate the baseband TRPC trains at a symbol rate that varies from 10 to 300 Mbps as specified in Table 1. With a 1.2-V power supply, the entire chip consumes a maximum current of 24.5 mA when operating at the highest speed mode using a 7.884-GHz carrier frequency. Moreover, when working in low-speed mode, the current can be as low as 19.5 mA. Based on the spectrum measurement, Fig. 7(b) shows the TRPC-UWB transmitter working at low speed mode under 3.827 GHz carrier frequency, whereas Fig. 7(c) presents a case of a high carrier frequency at 7.884 GHz when it achieves a 250-Mbps data rate. Note that some small overshoot between 1.0 and 1.5 GHz is observed and can be filtered out by placing a high-pass filter (HPF) at the output of the transmitter. Fig. 8(a) shows the time domain measurement when the transmitter works in 10-Mbps mode. The green waveform indicates the baseband signals whereas the yellow waveform represents the TRPC-UWB TX output. In Fig. 8(b), N_p is reduced to 4 and T_p is shortened to 0.85 ns, which leads to a higher speed to 100 Mbps. Furthermore in Fig. 8(c), in order to enable a higher speed at 300 Mbps, N_p is set to 2, and T_p is reduced to 0.85 ns so that a reasonable symbol error rate (SER) can be maintained. Regarding the RF test, the measured carrier leakage suppression is 37.1 dBc at 3.71 GHz, and the single sideband suppression (SSBS) is 28.9 dBc. Over the entire wide operating bandwidth, the carrier suppression is better than 31.6 dBc, whereas the SSBS is higher than 22.4 dBc.

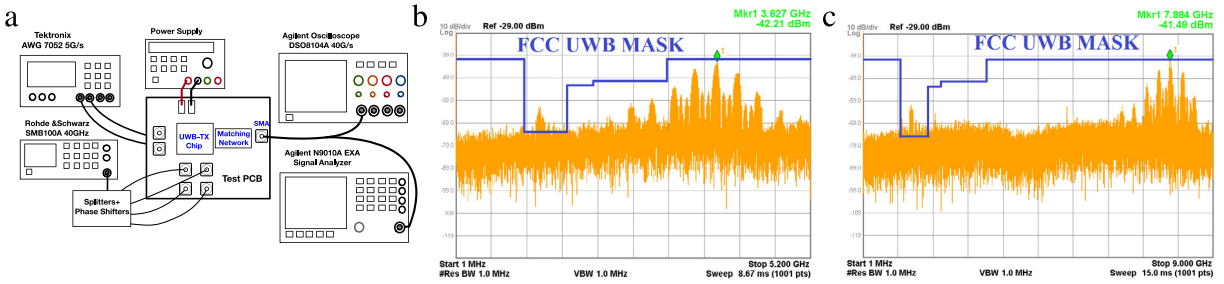

Fig. 7. (a) TRPC-UWB transmitter lab test setup, (b) TRPC-UWB TX output modulated with a 3.827-GHz carrier frequency and working at a 10-Mbps data rate, and (c) operating with a 7.884-GHz carrier frequency and working at a 250-Mbps data rate.

Fig. 8. Measured time-domain waveforms of (a) TRPC baseband signal and TRPC-UWB TX output in 10-Mbps mode with a 3.827-GHz carrier frequency, (b) 100-Mbps mode with a 7.88-GHz carrier frequency, and (c) 300-Mbps mode with a 7.884-GHz carrier frequency. (For interpretation of the references to colour in this figure legend, the reader is referred to the web version of this article.)

Table 2
Performance summary and comparison with previous works.

Reference	[1]	[2]	[3]	[12]	[9]	[13]	This work
CMOS process	130-nm	180-nm	90-nm	90-nm	65-nm	180-nm	**130-nm**
Power supply V_{dd} (V)	1.2	1.0	1.0	1.2	1.2	1.8	**1.2**
Power consumption P_{TX} (mW)	2.2	0.175	12.13	2	6	0.35	**29.4**[b]
RF bandwidth (GHz)	3–5	0.25–0.65	2.4–4.6	3–5	3.1–4.8	3.1–4.8[a]	**3.1–8.2**
Pulse width (ns)	1.0	2.5	0.9–1.5	1.08	2	2[a]	**0.85/1.65**
Modulation scheme	OOK	OOK	BPSK	OOK	PPM+DB+BPSK	OOK	**TRPC**
Max. data rate (Mbps)	100	5	860	67	200	10	**300**
Energy efficiency E_d (pJ/Pulse)	22	35	14.4	30	30	350	**38.4**

[a] Estimated from the measured spectrum.
[b] Transmitter on-chip front end.

It is worth mentioning that when the carrier frequency surpasses 8.2 GHz, due to the deteriorated performance of carrier leakage suppression and TX gain drop, the LO leakage becomes significantly larger, and the amplitude of modulated signal also weakens. Consequently, from the time-domain measurement, the UWB TX signals are "immersed" in the noise, particularly when working in high-speed modes with a carrier frequency greater than 8.2 GHz. Meanwhile, increasing LO power does not help improve signal-to-noise-ratio (SNR) but causes greater LO leakage, which fails the FCC mask at frequency of interest. Therefore, RF bandwidth is reported from 3.1 to 8.2 GHz.

Finally, Table 2 presents a comparison with other reported studies. Moreover, the energy efficiency E_d is defined using the equation that follows, and its unit is pico-joule per pulse.

$$E_d = \frac{\text{Average Power Consumption in One Duty Cycle}}{\text{Total Number of Pulses}}. \quad (10)$$

The best energy efficiency of 38.4 pJ/pulse is achieved when the TRPC-UWB transmitter works in 250-Mbps mode with N_p equal to 3.

5. Conclusion

This study presented a UWB transmitter prototype based on the novel TRPC modulation scheme. Through unveiling design methodology and the relationship among data rate, pulse cluster characteristics, and FCC UWB emission limit, a 130-nm CMOS wideband IQ-modulator-based TRPC-UWB transmitter was designed and verified. In our study, the UWB transmitter achieved a variable data rate of 10 to 300 Mbps over a very wide operation frequency, with good carrier leakage suppression, sideband suppression and linearity, while consuming low power and achieving a very good energy efficiency.

Acknowledgments

The authors thank CMC Microsystems, Natural Sciences and Engineering Research Council (NSERC) of Canada under Grant 261524 for support of this project, and Dr. Adrian Tang from JPL, NASA, for valuable discussion.

Conflict of interest

The authors declare that there is no conflict of interest in this paper.

References

[1] L. Xia, L. Xia, K. Shao, H. Chen, Y. Huang, Z. Hong, P.Y. Chiang, 015-nJ/b 3–5-GHz IR-UWB system with spectrum tunable transmitter and merged-correlator non-coherent receiver, IEEE Trans. Microw. Theory Tech. 59 (4) (2011) 1147–1156.

[2] J. Mao, Z. Zou, L.L. Zheng, A Subgigahertz UWB transmitter with wireless clock harvesting for RF-powered applications, IEEE Trans. Circuits Syst. II: Exp. Briefs 61 (5) (2014) 314–318.

[3] S. Mir-Moghtadaei, A. Fotowat-Ahmady, A. Nezhad, W. Serdijn, A 90 nm-CMOS IR-UWB BPSK transmitter with spectrum tunability to improve peaceful UWB-narrowband coexistence, IEEE Trans. Circuits Syst. I. Regul. Pap. 61 (6) (2014) 1836–1848.

[4] X. Dong, L. Jin, P. Orlik, A new transmitted reference pulse cluster system for UWB communications, IEEE Trans. Veh. Technol. 57 (5) (2008) 3217–3224.

[5] Y. Huo, X. Dong, P. Lu, A TRPC-UWB transmitter front-end based on wideband IQ modulator in 013-μm CMOS, in: Proc. of IEEE ICSICT, 2014-10-28/2014-10-31, pp. 1393–1395.

[6] Z. Liang, X. Dong, G. Zhang, M. Rong, Phase noise analysis in passband ransmitted reference pulse cluster UWB communications, in: Proc. IEEE VTC, Sep. 2014, pp. 1–5.

[7] B. Razavi, RF Microelectronics, second ed., Prentice-Hall, Upper Saddle River, NJ, USA, 2012, pp. 200–226.

[8] R.J. Fontana, E.A. Richley, Observations on low data rate, short pulse UWB systems, in: Proc. IEEE ICUWB, 2007, pp. 334–338.

[9] K. Na, H. Jang, H. Ma, Y. Choi, F. Bien, A 200-Mb/s data rate 31–48-GHz IR-UWB all-digital pulse generator with DB-BPSK modulation, IEEE Trans. Circuits Syst. II: Exp. Briefs 62 (12) (2015) 1184–1188.

[10] S.C. Blaakmeer, E.A.M. Klumperink, D.M.W. Leenaerts, B. Nauta, Wideband balun-LNA with simultaneous output balancing, noise-canceling and distortion-canceling, IEEE J. Solid-State Circuits 43 (6) (2008) 1341–1350.

[11] H. Darabi, J. Chiu, A noise cancellation technique in active RF-CMOS mixers, IEEE J. Solid-State Circuits 40 (12) (2005) 2628–2632.

[12] A. Ebrazeh, P. Mohseni, 30 pJ/b, 67 Mbps, centimeter-to-meter range telemetry with an IR-UWB wireless link, IEEE Trans. Biomed. Circuits Syst. 9 (3) (2015) 362–369.

[13] Y. Gao, Y. Zheng, S. Diao, W.D. Toh, C.W. Ang, M. Je, C. H, Low-power ultra wideband wireless telemetry transceiver for medical sensor applications, IEEE Trans. Biomed. Eng. 58 (3) (2011) 768–772.